Monthly Notices of the ROYAL ASTRONOMICAL SOCIETY

Mon. Not. R. Astron. Soc. **414,** 1508–1516 (2011) doi:10.1111/j.1365-2966.2011.18483.x

X-ray bursts and burst oscillations from the slowly spinning X-ray pulsar IGR J17480−2446 (Terzan 5)

S. Motta,[1,2]★ A. D'Aì,[3] A. Papitto,[4] A. Riggio,[4] T. Di Salvo,[3] L. Burderi,[5] T. Belloni,[1,2] L. Stella[6] and R. Iaria[3]

[1]*INAF - Osservatorio Astronomico di Brera, via E. Bianchi 46, I-23807 Merate (LC), Italy*
[2]*Università dell'Insubria, via Valleggio 11, I-22100 Como, Italy*
[3]*Dipartimento di Scienze Fisiche ed Astronomiche, Università di Palermo, via Archirafi 36, 90123 Palermo, Italy*
[4]*INAF - Osservatorio Astronomico di Cagliari, localitá Poggio dei Pini, strada 54, 09012 Capoterra, Italy*
[5]*Dipartimento di Fisica, Università degli Studi di Cagliari, SP Monserrato-Sestu, KM 0.7, 09042 Monserrato, Italy*
[6]*INAF - Osservatorio Astronomico di Roma, via di Frascati 33, I-00040 Monteporzio Catone Rome, Italy*

Accepted 2011 February 6. Received 2011 January 7; in original form 2010 November 28

ABSTRACT

The newly discovered 11-Hz accreting pulsar, IGR J17480−2446, located in the globular cluster Terzan 5, has shown several bursts with a recurrence time as short as a few minutes. The source shows the shortest recurrence time ever observed from a neutron star. Here we present a study of the morphological, spectral and temporal properties of 107 bursts observed by the *Rossi X-ray Timing Explorer*. The recurrence time and the fluence of the bursts clearly anticorrelate with the increase in the persistent X-ray flux. The ratio between the energy generated by the accretion of mass and that liberated during bursts indicates that helium is ignited in a hydrogen-rich layer. Therefore, we conclude that all the bursts shown by IGR J17480−2446 are Type I X-ray bursts. Pulsations could be detected in all the brightest bursts and no drifts of the frequency are observed within 0.25 Hz of the spin frequency of the neutron star. These are also phase-locked with respect to the pulsations observed during the persistent emission and no rise in the rms associated to the pulse frequency is observed during the burst. This behaviour would favour a scenario where the Type I burst, possibly ignited at the polar caps, immediately propagates to the entire neutron star surface.

Key words: pulsars: individual: IGR J17480−2446 – X-rays: binaries.

1 INTRODUCTION

Type I X-ray bursts result from the unstable thermonuclear ignition of the accreted material on the surface of weakly magnetized neutron stars (NSs) (see Lewin et al. 1976; Strohmayer & Bildsten 2006; Galloway et al. 2008, and references therein for reviews on the subject). This material is accreted through the Roche lobe overflow from a lower mass companion star [low-mass X-ray binary (LMXB)]. In systems exhibiting bursts, the temperature and pressure at the base of the accreted layer slowly increase until the nuclear energy generation rate becomes more sensitive to temperature perturbations than to the radiative cooling. At this point the resulting thermonuclear instability leads to the runaway burning of the matter that has been deposited since the previous burst. During the flash, over 90 per cent of the accreted hydrogen and helium is expected to burn into carbon and heavier elements (Woosley et al. 2004). For the next flash to occur, a fresh layer of hydrogen/helium must first be accreted.

X-ray bursts are observed in about half of the total population of LMXBs in the Galaxy, but only 15 sources from this sample show coherent pulsations (Galloway et al. 2010) at, or within a few Hz from, the spin frequency of the NS during the burst emission. To date, only five LMXBs show coherent pulsations both during the burst and during the persistent X-ray emission (SAX J1808.4−3658, XTE J1814−338, HETE J1900.1−2455, IGR J17511−3057 and the peculiar case of Aql X−1 that showed coherent pulsations with an extremely low duty cycle, see Altamirano et al. 2010 and references therein). The spin frequency in these sources is between 245–550 Hz.

Notwithstanding the great amount of observational facts collected in recent years, we still lack a clear understanding of the physical mechanism responsible for the onset of the burst oscillations. It would be important to understand why only ∼20 per cent of the bursting X-ray sources show pulsations and why a drift of the order of a few Hz of the burst oscillation frequency is often observed during some Type I bursts (Muno et al. 2002), while in accreting

★E-mail: sara.motta@brera.inaf.it

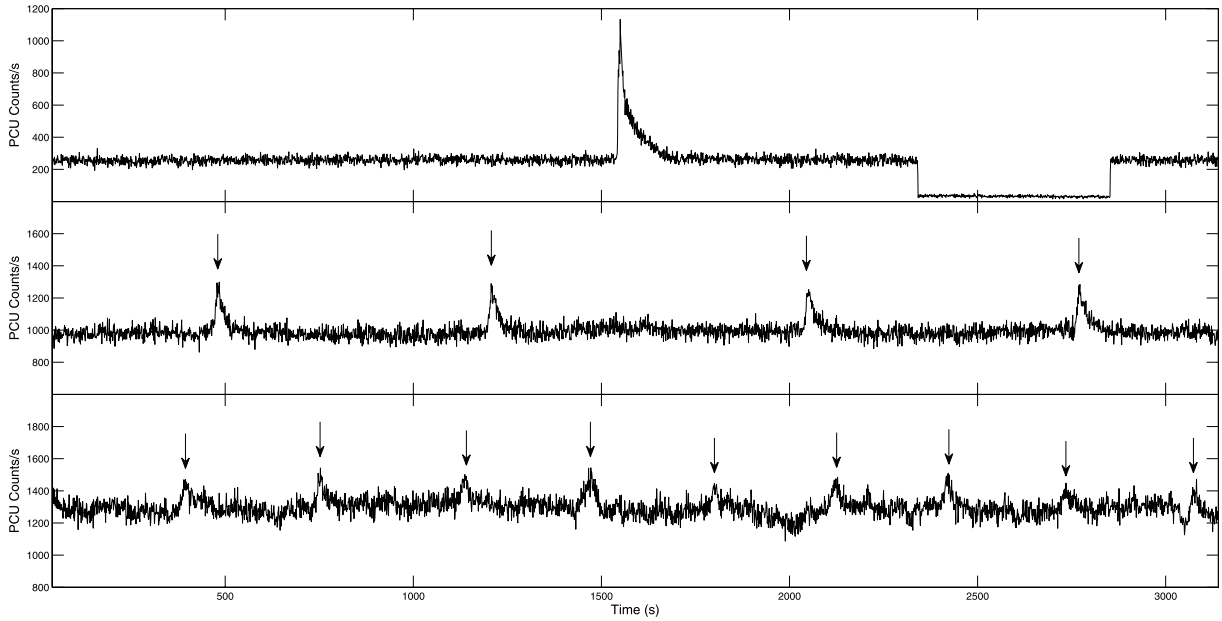

Figure 1. Light curves of three *RXTE* observations of IGR J17480−2446. For each observation, we plot the 1-s-resolution light curve from the beginning of the *RXTE* pointing. We show the first 3 ks for each observation. From the top to bottom panel: Obs. IDs 95437-01-01-00, 95437-01-02-01 and 95437-01-04-01, respectively. The arrows in the middle and bottom panels mark the positions of the bursts. Note that in Obs. ID 95437-01-01-00 a clear eclipse due to the moon occultation is visible (see Strohmayer, Markwardt & Pereira 2010). The recurrence time between bursts is clearly different between the second and third observations (see text).

millisecond pulsars this drift is less evident (e.g. Altamirano et al. 2010, and references therein).

The recent discovery of the 11-Hz accreting X-ray pulsar in the globular cluster Terzan 5, also showing burst oscillations at the same frequency, can be of immense help to shed light on these questions, definitely ruling out the need for high NS spin frequency as a necessary ingredient both for the onset of an X-ray burst and for the burst oscillations.

Furthermore, since the burst peak flux from IGR J17480−2446 is exceptionally low, compared to the values observed in other bursting sources, this source offers an excellent opportunity to study the effect of the hot NS contribution to the burst emission that arises when the burst luminosity is low compared to the persistent emission and in particular to the blackbody component (see van Paradijs & Lewin 1986).

2 OBSERVATIONS AND DATA ANALYSIS

INTEGRAL detected a transient source in the globular cluster Terzan 5 on 2010 October 10.365 (Bordas et al. 2010), tentatively attributed to the known LMXB transient EXO 1745−248. However, follow-up *Swift* observations refined the source position, excluding the association with EXO 1745−248; the new source was therefore dubbed as IGR J17480−2446. A *Chandra* observation confirmed the position of the source (see Pooley, Homan & Heinke 2010) and its non-association with EXO 1745−248. The distance to Terzan 5 has been estimated as 5.9 ± 0.5 kpc (Lanzoni et al. 2010), which is the value we consider in the following.

Subsequent *Rossi X-ray Timing Explorer* (*RXTE*) observations of IGR J17480−2446 showed coherent pulsations at 11 Hz and the presence of bursts and burst oscillations (Altamirano & Watts 2010; Strohmayer & Markwardt 2010). The timing analysis of the pulse period revealed how the system has an orbital period of 21.327 h and a companion star of mass between 0.4–1 $M_\odot$ (Strohmayer et al. 2010; Papitto et al. 2011).

In this work, we focus on the X-ray bursts observed in the rising phase of the outburst of IGR J17480−2446 with the *RXTE*. We consider observations from 2010 October 13 to 17 (MJD 55482 to 55486, Obs. ID from 95437-01-01-00 to 95437-01-04-01).

2.1 Outburst light curve, persistent emission and burst analysis

IGR J17480−2446 was observed daily by the *RXTE* starting from MJD 55482.01 (Obs. ID from 95437-01-01-00, 2010 October 13), 3 d after its discovery by *INTEGRAL*. A sample of the light curves observed with the *RXTE* is shown in Fig. 1. The count rate observed by the PCU2 of the Proportional Counter Array (PCA) during the *persistent* emission[1] rises from ∼250 (October 13.0) to ∼1300 count s^{-1} PCU^{-1} (October 16.7).

To evaluate the X-ray *persistent* flux just prior to each burst onset, we extracted spectra using only the PCU2 of the PCA (3.5–25 keV) over a time-interval of 32 s before $T_{\rm peak}$. We modelled the spectrum with the sum of a blackbody and a Comptonized component compps (Poutanen & Svensson 1996), and computed unabsorbed fluxes extrapolating in the 0.1–100 keV energy band. The source unabsorbed *persistent* flux rises from $F_{\rm pers} = 0.54(5) \times 10^{-8}$ erg cm^{-2} s^{-1} on October 13.0 to a peak value of $F_{\rm pers} = 1.7(2) \times 10^{-8}$ erg cm^{-2} s^{-1} during the last observation considered here (October 16.7).

X-ray bursts appearing at regular intervals are detected in all the *RXTE* observations we consider (October 13–16). The recurrence time between consecutive bursts decreases from $\gtrsim$24 min to

[1] Even though the source is an X-ray transient, we refer to the *persistent* emission as the main body of the outburst emission and to the *burst* emission when the source exhibits thermonuclear flashes.

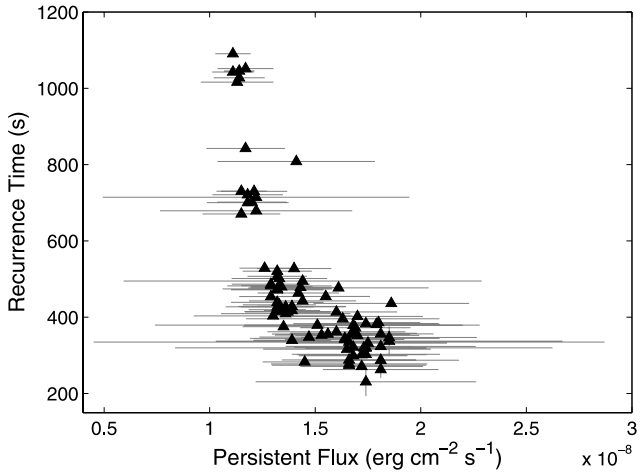

Figure 2. Variation in the recurrence time as a function of the *persistent* flux.

≃5 min, while the *persistent* flux increases (see Fig. 2). After October 17, the bursts disappeared to appear again on October 18. To analyse the morphological properties of the bursts observed during the rising part of the outburst, we consider background-subtracted light curves extracted from data taken in the Event (122-μs temporal resolution) and Good Xenon (1-μs temporal resolution) packing modes. Binning the light curves in 0.125 s intervals, we modelled the burst shape with a five-parameter model: persistent count rate, start time of the burst ($T_{\rm rise}$), peak time ($T_{\rm peak}$), amplitude of the burst and exponential decay time of the burst (τ). The model assumes a linear rise between $T_{\rm rise}$ and $T_{\rm peak}$, and an exponential decay after the peak. The bursts show a typical rise time between few and ∼20 s and an exponential decay time between ∼10 and ∼100 s. As an example we show in the top panel of Fig. 1 the shape of the first and most-energetic burst observed by the *RXTE* and in the following panels the typical shapes of the subsequent fainter bursts.

To verify possible photospheric radius expansion episodes during the bursts, we extracted PCU2 spectra of the brightest burst over time-intervals 2 s long and modelled them with an absorbed blackbody. The best-fitting values of the blackbody temperature and radius are plotted in the middle and lower panels of Fig. 3, respectively. The apparent radius observed at infinity has a constant value of $R_{\rm app}^{\infty} = (3.3 \pm 0.5) d_{5.9}$ km, clearly indicating that no radius expansion takes place. The apparent radius has subsequently been converted into an effective radius, taking into account the hardening factor and the effect of the gravitational redshift (see Section 3 for details). We also measured the mean apparent radii for selected bursts following the first brightest one (see Table 1). To do this, we followed Sztajno et al. (1986). For each selected burst, we made a two-component fit to the combined persistent and burst emission, involving a blackbody component (associated to the NS emission) and a Comptonized component that represents the emission which is promptly radiated upon the accretion of matter. We assumed that the latter component is not affected by the occurrence of a thermonuclear flash and we adopted the apparent blackbody radius associated to the other component as the mean radius of the region emitting the blackbody radiation during the Type I X-ray bursts. To better constrain the parameters of the persistent emission spectrum, we extracted the persistent emission spectrum immediately before the burst occurrence and we fitted it. We then used this template model to fit the emission during the bursts, keeping the parameters of the Comptonization component constant and leaving the parameters of the blackbody component free to vary. The resulting measures (where the corrections adopted for the first burst have been applied) are listed in Table 1.

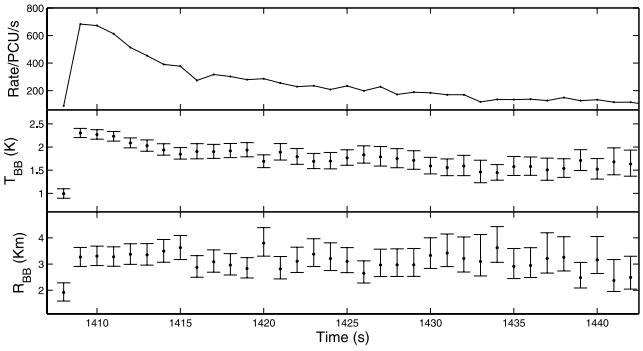

Figure 3. Top panel: light curve of the strongest burst, observed on MJD 55482. Middle and bottom panels: evolution of the radius and temperature of the best-fitting blackbody component. The integration time of the points is 2 s at the peak and 4 s during the last part of the decay.

Table 1. Mean temperature and radius of the blackbody component associated to the thermonuclear burst emission. The upper and lower limits to the radius are corrected for the hardening factor $f_{\rm c}$ and for the gravitational redshift contribution.

Number	T (keV)	$R_{\rm min}$ (km)	$R_{\rm max}$ (km)
2	$1.41^{+0.03}_{-0.08}$	8.36	19.08
6	$1.34^{+0.07}_{-0.08}$	9.26	21.12
10	$1.36^{+0.08}_{-0.10}$	8.31	19.01
28	$1.27^{+0.04}_{-0.06}$	10.60	25.00
31	$1.37^{+0.03}_{-0.06}$	9.42	22.77
32	$1.28^{+0.06}_{-0.06}$	10.19	24.40
80	$1.17^{+0.05}_{-0.01}$	14.56	35.24
93	$1.17^{+0.01}_{-0.03}$	14.86	34.66
106	$1.17^{+0.03}_{-0.03}$	14.82	34.29

To verify our results, we attempted to stack data from several faint bursts observed at higher accretion rates (MJD 55485) and applied the same procedure followed for the single bursts. Analysing the profiles of the fainter bursts, both rise and decay times often appeared different from one burst to another. For this reason, we selected bursts with similar profiles (i.e. similar rise and decay times) and averaged their spectra in order to obtain the measure of the mean radius and temperature of the blackbody emitting region. We obtained values consistent with the ones reported in Table 1.

The energetics of each burst have been evaluated by extracting a PCU2 spectrum taken in a fast timing mode (Generic Event and Good Xenon) over a time-range containing the whole burst and of a variable length depending on τ and on the variability of the *persistent* flux. We subtracted as the background the spectrum of the persistent emission, extracted over an interval of 32 s before the onset of the burst ($T_{\rm rise}$). We modelled the resulting spectrum with an absorbed blackbody. The fluence estimates we obtain in the 0.1–100 keV band are listed in Table 2. The first burst is the most energetic, showing a bolometric fluence of

Table 2. Properties of the 107 X-ray bursts from IGR J17480−2446. Columns are: (1) burst number, (2) Obs. ID, (3) start time (MJD, referred to the Solar system centre of mass), (4) recurrence time, (5) rise time, (6) decay time τ, (7) persistent flux, (8) burst fluence, (9) ratio of the integrated persistent flux to the burst fluence (α) and (10) predicted recurrence time (assuming the energy conversion efficiency equal to $\sim$2 MeV per nucleon).

Serial number	Obs. ID	$T_{\rm start}$ (MJD)	$T_{\rm rec}$ (s)	$t_{\rm rise}$ (s)	τ (s)	Persistent flux (10^{-8} erg cm^{-2} s^{-1})	Burst fluence (10^{-8} erg cm^{-2})	α	$T_{\rm rec}^{\rm pred}$ (s)
(1)	(2)	(3)	(4)	(5)	(6)	(7)	(8)	(9)	(10)
1	95437-01-01-00	55482.03	–	5.0 ± 0.1	34 ± 1	0.52 ± 0.01	31.5 ± 0.6	–	6448 ± 167
2	95437-01-02-00	55483.20	–	7 ± 1	23 ± 3	1.13 ± 0.08	15.7 ± 1.1	–	1470 ± 147
3	95437-01-02-00	55483.21	1052 ± 1	11 ± 1	17 ± 3	1.17 ± 0.13	13.4 ± 1.5	92 ± 10	1212 ± 193
4	95437-01-02-00	55483.22	1016 ± 2	11 ± 2	20 ± 2	1.13 ± 0.17	12.5 ± 1.9	92 ± 14	1171 ± 252
5	95437-01-02-00	55483.26	–	9 ± 1	21 ± 3	1.10 ± 0.15	12.0 ± 1.7	–	1154 ± 227
6	95437-01-02-00	55483.27	1043 ± 1	12 ± 1	16 ± 3	1.11 ± 0.10	12.2 ± 1.1	95 ± 8	1163 ± 147
7	95437-01-02-00	55483.28	1090 ± 1	8 ± 1	22 ± 3	1.11 ± 0.08	13.6 ± 1.0	89 ± 7	1297 ± 139
8	95437-01-02-00	55483.33	–	12 ± 1	25 ± 3	1.15 ± 0.08	14.4 ± 1.0	–	1325 ± 129
9	95437-01-02-00	55483.34	1028 ± 1	10 ± 1	17 ± 2	1.14 ± 0.12	10.2 ± 1.1	115 ± 12	947 ± 142
10	95437-01-02-00	55483.35	1045 ± 2	11 ± 2	17 ± 2	1.14 ± 0.07	12.4 ± 0.8	96 ± 6	1151 ± 103
11	95437-01-02-01	55483.72	–	17 ± 2	16 ± 2	1.17 ± 0.13	10.1 ± 1.1	–	914 ± 140
12	95437-01-02-01	55483.73	730 ± 3	14 ± 2	21 ± 3	1.15 ± 0.12	10.4 ± 1.1	81 ± 8	957 ± 140
13	95437-01-02-01	55483.74	842 ± 3	13 ± 2	20 ± 2	1.17 ± 0.19	6.8 ± 1.1	146 ± 23	612 ± 137
14	95437-01-02-01	55483.75	721 ± 2	12 ± 2	21 ± 3	1.18 ± 0.17	5.7 ± 0.8	148 ± 21	514 ± 103
15	95437-01-02-01	55483.78	–	14 ± 2	15 ± 3	1.23 ± 1.53	4.3 ± 5.4	–	371 ± 653
16	95437-01-02-01	55483.79	700 ± 2	14 ± 1	14 ± 2	1.18 ± 0.19	8.4 ± 1.4	99 ± 16	753 ± 175
17	95437-01-02-01	55483.80	702 ± 2	9 ± 1	18 ± 2	1.20 ± 0.16	7.8 ± 1.1	109 ± 15	684 ± 132
18	95437-01-02-01	55483.81	679 ± 2	16 ± 2	13 ± 2	1.22 ± 0.45	3.9 ± 1.4	215 ± 80	335 ± 176
19	95437-01-02-01	55483.85	–	15 ± 2	10 ± 2	1.18 ± 0.35	3.3 ± 1.0	–	300 ± 126
20	95437-01-02-01	55483.86	671 ± 3	9 ± 2	21 ± 3	1.15 ± 0.18	5.2 ± 0.8	147 ± 24	481 ± 109
21	95437-01-02-01	55483.86	730 ± 3	12 ± 2	19 ± 3	1.21 ± 0.16	7.5 ± 1.0	119 ± 15	652 ± 120
22	95437-01-02-01	55483.87	714 ± 2	15 ± 1	17 ± 2	1.22 ± 0.73	8.4 ± 5.0	103 ± 61	733 ± 618
23	95437-01-03-00	55484.44	–	4 ± 0	12 ± 2	1.24 ± 0.20	8.0 ± 1.3	–	680 ± 158
24	95437-01-03-00	55484.44	501 ± 2	12 ± 2	13 ± 3	1.33 ± 0.23	4.4 ± 0.7	153 ± 26	346 ± 83
25	95437-01-03-00	55484.45	521 ± 4	15 ± 3	16 ± 3	1.32 ± 0.16	7.9 ± 1.0	87 ± 11	633 ± 111
26	95437-01-03-00	55484.46	529 ± 5	11 ± 4	17 ± 3	1.26 ± 0.12	6.2 ± 0.6	107 ± 10	522 ± 70
27	95437-01-03-00	55484.46	487 ± 6	17 ± 5	14 ± 4	1.29 ± 0.18	4.0 ± 0.6	159 ± 23	324 ± 66
28	95437-01-03-01	55484.57	–	12 ± 3	19 ± 4	1.36 ± 0.31	4.5 ± 1.0	–	347 ± 112
29	95437-01-03-01	55484.58	439 ± 4	13 ± 2	20 ± 5	1.32 ± 0.22	4.7 ± 0.8	124 ± 21	374 ± 88
30	95437-01-03-01	55484.59	482 ± 3	9 ± 1	25 ± 4	1.33 ± 0.25	6.2 ± 1.2	104 ± 19	491 ± 129
31	95437-01-03-01	55484.59	483 ± 3	14 ± 2	16 ± 3	1.29 ± 0.14	7.2 ± 0.8	86 ± 9	593 ± 92
32	95437-01-03-01	55484.60	454 ± 3	16 ± 2	13 ± 2	1.29 ± 0.15	5.2 ± 0.6	114 ± 13	423 ± 70
33	95437-01-03-02	55484.63	–	15 ± 3	32 ± 5	1.34 ± 0.31	7.9 ± 1.8	–	626 ± 206
34	95437-01-03-02	55484.63	472 ± 4	14 ± 2	14 ± 3	1.32 ± 0.22	4.6 ± 0.8	135 ± 22	370 ± 87
35	95437-01-03-02	55484.64	480 ± 3	13 ± 2	11 ± 3	1.34 ± 0.15	5.2 ± 0.6	124 ± 14	411 ± 63
36	95437-01-03-02	55484.65	507 ± 3	8 ± 2	29 ± 20	1.32 ± 0.14	8.3 ± 0.9	80 ± 9	669 ± 101
37	95437-01-03-02	55484.65	474 ± 11	15 ± 11	18 ± 6	1.32 ± 0.26	4.0 ± 0.8	156 ± 31	321 ± 89
38	95437-01-03-02	55484.66	420 ± 14	54 ± 9	113 ± 32	1.32 ± 0.13	8.0 ± 0.8	69 ± 7	645 ± 93
39	95437-01-03-02	55484.66	528 ± 9	19 ± 2	22 ± 4	1.40 ± 0.18	8.2 ± 1.0	90 ± 11	621 ± 110
40	95437-01-03-03	55484.76	–	18 ± 7	10 ± 3	1.53 ± 0.86	6.7 ± 3.7	–	462 ± 367
41	95437-01-03-03	55484.76	379 ± 8	91 ± 4	92 ± 2	1.51 ± 0.77	5.9 ± 3.0	98 ± 50	411 ± 296
42	95437-01-03-03	55484.77	495 ± 5	13 ± 2	7 ± 2	1.44 ± 0.85	5.8 ± 3.4	122 ± 72	429 ± 357
43	95437-01-03-03	55484.77	463 ± 2	3 ± 1	41 ± 5	1.42 ± 0.19	6.7 ± 0.9	99 ± 13	496 ± 95
44	95437-01-03-03	55484.78	418 ± 5	25 ± 5	74 ± 18	1.39 ± 0.13	7.4 ± 0.7	79 ± 8	560 ± 76
45	95437-01-03-03	55484.78	477 ± 6	10 ± 3	19 ± 5	1.61 ± 0.43	4.6 ± 1.2	168 ± 45	300 ± 113
46	95437-01-03-03	55484.79	454 ± 4	20 ± 3	11 ± 3	1.55 ± 0.21	5.7 ± 0.8	124 ± 17	388 ± 74
47	95437-01-03-03	55484.79	478 ± 4	13 ± 3	19 ± 4	1.43 ± 0.17	6.2 ± 0.8	110 ± 13	460 ± 79
48	95437-01-03-03	55484.82	–	12 ± 4	20 ± 5	1.42 ± 0.41	4.1 ± 1.2	–	306 ± 123
49	95437-01-03-03	55484.83	353 ± 11	51 ± 10	12 ± 4	1.53 ± 0.22	4.1 ± 0.6	131 ± 19	286 ± 59
50	95437-01-03-03	55484.83	427 ± 11	39 ± 4	46 ± 9	1.32 ± 0.17	8.0 ± 1.0	71 ± 9	638 ± 118
51	95437-01-03-03	55484.84	415 ± 6	23 ± 3	14 ± 4	1.34 ± 0.18	5.7 ± 0.7	98 ± 13	447 ± 83
52	95437-01-03-03	55484.84	403 ± 4	3 ± 1	82 ± 17	1.30 ± 0.38	3.4 ± 1.0	155 ± 45	275 ± 113
53	95437-01-03-03	55484.85	409 ± 3	19 ± 3	10 ± 2	1.36 ± 0.31	5.4 ± 1.2	103 ± 23	419 ± 134
54	95437-01-03-03	55484.85	432 ± 6	24 ± 5	37 ± 5	1.33 ± 0.17	7.1 ± 0.9	81 ± 11	566 ± 104
55	95437-01-03-03	55484.86	429 ± 6	4 ± 3	48 ± 13	1.33 ± 0.10	6.7 ± 0.5	86 ± 7	531 ± 59
56	95437-01-03-03	55484.89	–	4 ± 4	34 ± 7	1.39 ± 0.08	7.1 ± 0.4	–	540 ± 46
57	95437-01-03-03	55484.90	808 ± 5	10 ± 3	14 ± 4	1.41 ± 0.37	5.2 ± 1.4	218 ± 58	392 ± 147
58	95437-01-03-03	55484.90	414 ± 4	7 ± 3	45 ± 10	1.37 ± 0.20	5.7 ± 0.8	100 ± 15	440 ± 92

Table 2 – *continued*

Serial number	Obs. ID	$T_{\rm start}$ (MJD)	$T_{\rm rec}$ (s)	$t_{\rm rise}$ (s)	τ (s)	Persistent flux (10^{-8} erg cm^{-2} s^{-1})	Burst fluence (10^{-8} erg cm^{-2})	α	$T_{\rm rec}^{\rm pred}$ (s)
(1)	(2)	(3)	(4)	(5)	(6)	(7)	(8)	(9)	(10)
59	95437-01-03-03	55484.91	428 ± 15	54 ± 14	58 ± 15	1.39 ± 0.25	5.0 ± 0.9	120 ± 22	379 ± 98
60	95437-01-03-03	55484.91	427 ± 15	17 ± 4	9 ± 4	1.36 ± 0.28	5.5 ± 1.2	105 ± 22	430 ± 128
61	95437-01-03-03	55484.91	375 ± 5	43 ± 4	18 ± 4	1.35 ± 0.19	5.9 ± 0.9	86 ± 12	464 ± 94
62	95437-01-03-03	55484.92	443 ± 5	10 ± 4	111 ± 18	1.44 ± 0.25	6.5 ± 1.1	98 ± 17	477 ± 119
63	95437-01-04-00	55485.41	–	27 ± 4	9 ± 4	1.41 ± 0.22	4.4 ± 0.7	–	330 ± 73
64	95437-01-04-00	55485.42	340 ± 4	13 ± 2	14 ± 3	1.39 ± 0.18	4.7 ± 0.6	100 ± 13	358 ± 67
65	95437-01-04-00	55485.42	283 ± 5	32 ± 5	9 ± 3	1.45 ± 0.20	4.6 ± 0.6	88 ± 12	339 ± 66
66	95437-01-04-00	55485.43	356 ± 6	40 ± 3	146 ± 15	1.56 ± 0.26	5.2 ± 0.9	107 ± 18	353 ± 85
67	95437-01-04-00	55485.43	396 ± 4	17 ± 3	10 ± 3	1.63 ± 0.46	4.8 ± 1.3	134 ± 38	312 ± 124
68	95437-01-04-00	55485.44	414 ± 4	12 ± 3	23 ± 5	1.60 ± 0.29	4.8 ± 0.9	137 ± 25	320 ± 82
69	95437-01-04-00	55485.44	362 ± 5	15 ± 4	20 ± 4	1.60 ± 0.33	2.5 ± 0.5	234 ± 48	163 ± 47
70	95437-01-04-00	55485.44	274 ± 7	51 ± 6	17 ± 4	1.66 ± 0.37	1.6 ± 0.4	285 ± 63	102 ± 32
71	95437-01-04-00	55485.45	348 ± 12	50 ± 11	8 ± 3	1.47 ± 0.23	2.0 ± 0.3	253 ± 42	145 ± 33
72	95437-01-04-00	55485.48	–	35 ± 4	516 ± 99	1.57 ± 0.46	2.1 ± 0.6	–	141 ± 58
73	95437-01-04-00	55485.49	402 ± 5	14 ± 3	18 ± 4	1.70 ± 0.31	5.0 ± 0.9	137 ± 25	310 ± 80
74	95437-01-04-00	55485.49	342 ± 4	18 ± 3	30 ± 7	1.64 ± 0.28	7.3 ± 1.2	77 ± 13	469 ± 114
75	95437-01-04-00	55485.50	353 ± 4	13 ± 3	19 ± 4	1.70 ± 0.29	4.5 ± 0.8	134 ± 23	279 ± 68
76	95437-01-04-00	55485.50	288 ± 6	20 ± 5	13 ± 3	1.66 ± 0.32	3.5 ± 0.7	138 ± 27	221 ± 60
77	95437-01-04-00	55485.50	335 ± 7	34 ± 5	16 ± 8	1.66 ± 1.21	4.1 ± 3.0	135 ± 98	263 ± 271
78	95437-01-04-00	55485.51	358 ± 6	14 ± 4	27 ± 9	1.68 ± 0.30	5.4 ± 1.0	112 ± 20	338 ± 85
79	95437-01-04-00	55485.51	278 ± 8	32 ± 7	29 ± 9	1.66 ± 0.37	3.8 ± 0.8	121 ± 27	242 ± 76
80	95437-01-04-01	55485.55	–	15 ± 3	43 ± 7	1.65 ± 0.42	4.2 ± 1.1	–	269 ± 96
81	95437-01-04-01	55485.56	356 ± 3	17 ± 1	111 ± 33	1.67 ± 0.28	4.0 ± 0.7	149 ± 25	252 ± 59
82	95437-01-04-01	55485.56	381 ± 3	27 ± 3	10 ± 5	1.79 ± 0.30	4.3 ± 0.7	161 ± 27	251 ± 60
83	95437-01-04-01	55485.56	320 ± 5	47 ± 4	9 ± 2	1.73 ± 0.89	4.4 ± 2.3	125 ± 65	270 ± 197
84	95437-01-04-01	55485.57	345 ± 8	24 ± 7	42 ± 7	1.64 ± 0.45	3.2 ± 0.9	175 ± 48	208 ± 81
85	95437-01-04-01	55485.57	322 ± 8	20 ± 5	48 ± 17	1.68 ± 0.28	5.3 ± 0.9	102 ± 17	333 ± 78
86	95437-01-04-01	55485.57	299 ± 6	24 ± 5	14 ± 3	1.68 ± 0.26	3.8 ± 0.6	134 ± 21	237 ± 51
87	95437-01-04-01	55485.58	316 ± 5	18 ± 3	33 ± 12	1.65 ± 0.40	5.2 ± 1.2	101 ± 24	331 ± 113
88	95437-01-04-01	55485.61	–	13 ± 3	32 ± 8	1.64 ± 0.27	4.8 ± 0.6	–	310 ± 52
89	95437-01-04-01	55485.61	287 ± 5	39 ± 4	32 ± 10	1.81 ± 0.37	3.7 ± 0.8	141 ± 29	216 ± 63
90	95437-01-04-01	55485.61	302 ± 7	28 ± 6	92 ± 24	1.72 ± 0.31	8.0 ± 1.4	65 ± 12	494 ± 124
91	95437-01-04-01	55485.62	347 ± 6	17 ± 3	16 ± 4	1.85 ± 0.42	4.4 ± 1.0	147 ± 33	249 ± 79
92	95437-01-04-01	55485.62	321 ± 4	22 ± 2	19 ± 4	1.74 ± 0.19	6.0 ± 0.7	92 ± 10	368 ± 57
93	95437-01-04-01	55485.63	303 ± 5	18 ± 4	48 ± 15	1.74 ± 0.35	5.1 ± 1.0	102 ± 21	313 ± 89
94	95437-01-04-01	55485.63	356 ± 6	17 ± 5	36 ± 7	1.81 ± 0.25	6.3 ± 0.9	102 ± 14	369 ± 72
95	95437-01-04-01	55485.63	319 ± 6	23 ± 3	19 ± 4	1.74 ± 0.29	7.1 ± 1.2	78 ± 13	432 ± 101
96	95437-01-04-01	55485.64	271 ± 6	50 ± 5	20 ± 5	1.72 ± 0.29	6.8 ± 1.1	69 ± 12	418 ± 100
97	95437-01-04-01	55485.64	332 ± 8	24 ± 5	19 ± 5	1.75 ± 0.37	4.0 ± 0.9	145 ± 31	242 ± 73
98	95437-01-04-01	55485.64	323 ± 6	17 ± 3	9 ± 3	1.81 ± 0.45	4.7 ± 1.2	126 ± 31	273 ± 96
99	95437-01-04-01	55485.68	–	40 ± 6	15 ± 3	1.78 ± 0.39	4.4 ± 1.0	–	262 ± 81
100	95437-01-04-01	55485.68	373 ± 6	5 ± 1	41 ± 9	1.69 ± 0.26	7.9 ± 1.2	79 ± 12	497 ± 108
101	95437-01-04-01	55485.68	383 ± 3	14 ± 3	42 ± 7	1.74 ± 0.34	6.5 ± 1.3	102 ± 20	397 ± 111
102	95437-01-04-01	55485.69	263 ± 22	110 ± 22	45 ± 20	1.81 ± 0.27	8.9 ± 1.3	54 ± 9	519 ± 111
103	95437-01-04-01	55485.69	379 ± 22	24 ± 5	26 ± 9	1.68 ± 0.52	3.2 ± 1.0	200 ± 63	201 ± 87
104	95437-01-04-01	55485.70	231 ± 38	95 ± 37	32 ± 9	1.74 ± 0.52	3.6 ± 1.1	111 ± 38	221 ± 94
105	95437-01-04-01	55485.70	337 ± 38	81 ± 8	34 ± 8	1.85 ± 0.82	3.3 ± 1.5	189 ± 87	189 ± 119
106	95437-01-04-01	55485.70	436 ± 8	15 ± 3	17 ± 3	1.86 ± 0.37	5.0 ± 1.0	161 ± 32	287 ± 80
107	95437-01-04-01	55485.71	386 ± 4	7 ± 3	37 ± 6	1.80 ± 0.20	6.0 ± 0.7	116 ± 13	353 ± 55

$\mathcal{F}_{\rm burst} = 3.15(6) \times 10^{-7}$ erg cm^{-2}. As the *persistent* flux of the source increases, bursts become more frequent and less energetic as $\sim$3.5 d after the first observation they have fluences of the order of $\sim 1 \times 10^{-8}$ erg cm^{-2} (see Fig. 1). We have then evaluated the ratio of the integrated persistent flux to the burst fluence, $\alpha = F_{\rm pers} t_{\rm rec}/\mathcal{F}_{\rm burst}$ for each burst for which the recurrence time could be unambiguously defined. Modelling the observed values with a constant α, we obtain an average value of $\langle\alpha\rangle = 96 \pm 3$, with a small variance of 1.32 over 89 points (see Fig. 4). As we discuss in the following, such values are compatible with a thermonuclear origin of the bursts (see also Chakraborty & Bhattacharyya 2011). To secure such an identification, we searched for the evidence of the spectral softening during the tails of the bursts, which could be interpreted as the cooling of the burst emission. While there is an indication of such a cooling during the first and brightest burst (see the middle panel of Fig. 3), a similar trend could not be observed for the subsequent, fainter bursts (see Galloway & in't Zand 2010; Chakraborty & Bhattacharyya 2011). We argue that this is not due to the absence of the softening, but due to the intrinsic difficulty in disentangling the persistent and the burst emission when the tail of the burst is immediately dominated

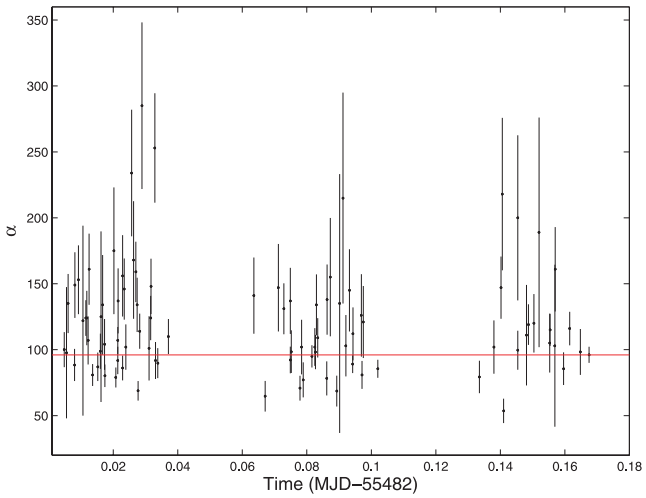

Figure 4. Values of α obtained for all the consecutive bursts. The horizontal line marks the mean value $\langle\alpha\rangle = 96 \pm 3$.

by the persistent emission. Furthermore, as pointed out by Sztajno et al. (1986) and van Paradijs & Lewin (1986), the spectral analysis of X-ray bursts is systematically affected if the persistent emission contains a spectral component which originates from the outer layer of a hot NS, which also transfers an important energetic contribution to the burst emission. In this situation, the net burst emission (i.e. excess above the persistent emission) is the difference between two blackbody spectra at different temperatures, corresponding to the total emission from the hot NS at different times. As a consequence, the net emission does not have a blackbody spectral distribution; therefore, a *standard* blackbody spectral analysis on the net burst emission is not decisive in the identification of the burst nature.

2.2 Burst oscillations

A burst-oscillation analysis was conducted using PCA data in the Good Xenon mode (for Obs. ID 95437-01-01-00) and Event mode (for the following observations), which provide the full timing and spectral information. We produced a dynamical power density spectrum (DPDS) by computing fast Fourier transforms of overlapping windows of data of length 4 s, stepped by 0.25 s (see Fig. 5, second panel from the top). As an example we show the DPDS for the case of the first burst observed on October 13. In the third panel from the top (Fig. 5), we show the evolution of the 11-Hz Leahy power (Leahy, Elsner & Weisskopf 1983) as a function of the time for that burst. Here the rise in the pulsation power during the burst is driven by the increase in the count rate. The increase is consistent with a constant fractional rms, as shown in the bottom panel of Fig. 5. We note that no drifting of the pulsation frequency is observed within 0.25 Hz from the best-fitting spin period. Interestingly, while the decay phase of the burst follows the expected exponential profile, the evolution of the power (see Fig. 5, third panel from the top) clearly shows a multipeak structure that does not reflect the decay in the light curve. A similar case in observed in XTE J1814−338 (Strohmayer et al. 2003).

The other bursts also show an increase (although statistically less evident) in the pulsation power. In particular, we observed a stronger power in the 11-Hz pulsations in bursts taking place during MJD 55482 and 55483. Later in the outburst, the increase in the power becomes difficult to observe as the bursts become fainter. This effect is likely due to the lack of statistics encountered when the net burst

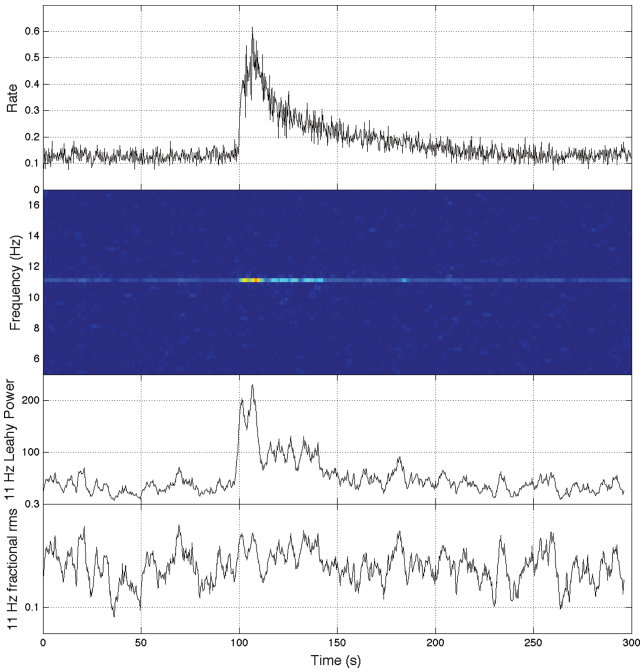

Figure 5. Analysis of the burst observed on October 13. From the top to bottom panel: light curve, DPDS, evolution of the Leahy power at 11.125 Hz and the corresponding fractional rms, respectively .

count rate decreases (making detections statistically weaker) as the persistent flux rises.

In order to ascertain the phase relation between the coherent pulsations observed during the *persistent* emission and burst oscillations, we reconstructed pulse profiles over 100-s-long intervals before each burst and over 20-s-long intervals after the bursts' onset. We performed an epoch folding around the best estimate of the spin period (see Papitto et al. 2011) for the two intervals, obtaining two pulse profiles that were fitted according to a standard harmonic decomposition. We then obtained the phase difference between the two profiles and studied the variations in the phase difference for each burst as a function of time. Such difference is in general consistent with zero for all examined bursts (Fig. 6). Considering the uncertainties in the phase estimates, we thus conclude that the burst oscillations originate from a region which is very close to the NS polar caps.

3 DISCUSSION AND CONCLUSIONS

In this paper, we report on the bursting behaviour of the newly discovered X-ray pulsar IGR J17480−2446.

The observed spin period and the magnetic field estimated for IGR J17480−2446 (see Papitto et al. 2011) place this source in between the population of classical ($B \gtrsim 10^{11}$ G, $P \geq 0.1$ s) and millisecond accreting X-ray pulsars ($B = 10^8$–10^9 G, $P = 1.5$–10 ms). This source therefore constitutes a *bona fide* candidate as a link between these two groups, being a slow, probably mildly recycled, pulsar. IGR J17480−2446 is presently the bursting source with the longest spin period observed.

To convert the flux into luminosity and the fluence into energy, we assumed the geometric isotropy of the emission and a source distance of 5.9 kpc. We further express this quantity in units of the Eddington luminosity (1.8×10^{38} erg s^{-1} for a 1.4-M$_\odot$ NS). From MJD 55482.00872 to 55486.56326, the source *persistent* luminosity rises from $\sim 2.2 \times 10^{37} d_{5.9}^2$ to $\sim 7.5 \times 10^{37} d_{5.9}^2$ erg s^{-1}. From these

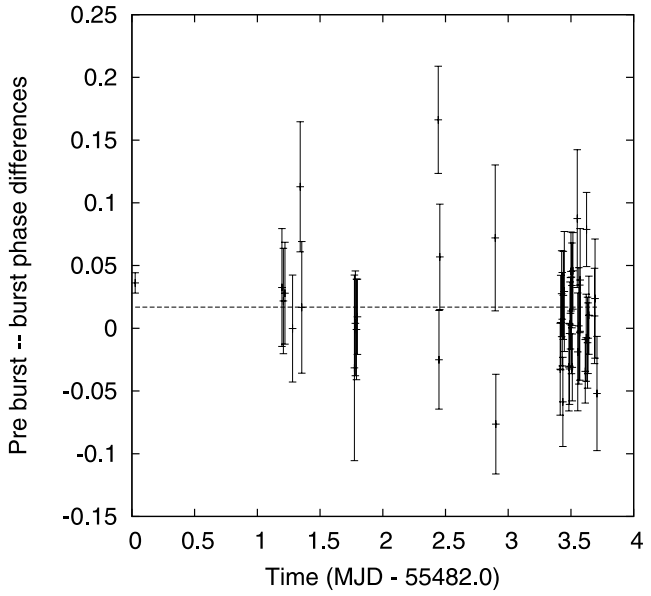

Figure 6. Phase difference between the pulse in the persistent emission and during the burst period.

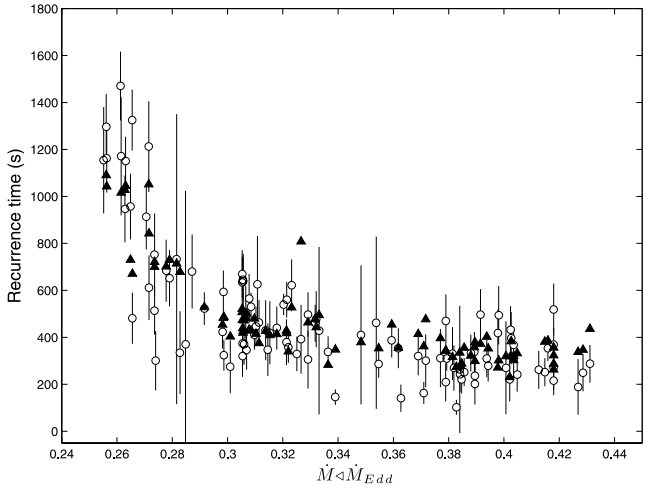

Figure 7. Observed (triangles) and predicted (circles) recurrence times plotted as a function of the measured local accretion rate. Error bars related to the accretion rate are not reported for clarity.

values, we infer an increase in the mass-accretion rate[2] from 0.1 to $0.37\dot{M}_{\rm Edd}$ (see Fig. 7). Consistent with this behaviour, the bursts become more frequent and fainter.

In this paper, we report on the analysis of 107 X-ray bursts shown by IGR J17480−2446 during the first 4 d of the *RXTE* monitoring. Since the *persistent* bolometric X-ray luminosity rises by a factor of ∼4 during this interval, we were able to study the properties of bursts at different mass-accretion rates.

The observed bursts have different profiles in the light curve. The rise time varies between few and ∼20 s, while the decay time (τ) falls in the range ∼20 to ∼100 s. The first, more intense bursts (MJD 55483 and 55484) show a typical Type I X-ray burst profile, featuring a linear rise and an exponential decay following the burst peak. The subsequent fainter bursts present a less clear profile, with rise times in some cases similar to the decay times. For some of the fainter bursts, a clear modelling of the profile was difficult, because the excursion in the intensity above the continuum due to the burst occurrence was comparable with the persistent emission variations.

The pulsation does not show any drifting of the frequency during the decay phase of the bursts. This phenomenon is also observed in bursting millisecond pulsars (XTE J1814−338, Markwardt & Swank 2003; HETE J1900.1−2455, Kaaret et al. 2006; IGR J17511−3057, Altamirano et al. 2010) and can be explained in terms of a non-significant expansion of the NS atmosphere during the thermonuclear combustion. Studying the spectral evolution during the first burst, no photospheric radius expansion is indeed observed (see Fig. 3).

Burst oscillations are always phase-locked within 0.2 phase units, indicating how the ignition begins in a region not far from the NS polar caps. The radius inferred from the spectral fitting for the first and most-intense burst is 3.2 ± 0.5 km. Also taking into account the corrective factors to translate this value into a physical size on the NS surface (see below), the obtained radius is compatible, within the uncertainties, with the NS radius.

The recurrence time of X-ray bursts was observed to decrease from ≥26 min to ≃5 min in anticorrelation with the persistent X-ray flux. The shortest recurrence time of X-ray bursts observed so far in IGR J17480−2446 is 3.3 min and it is seen in MJD 55487 (Obs. ID 95437-01-06-00, not considered in this work). The shortest recurrence time previously reported is 3.8 min (see Keek et al. 2010).

The very short recurrence time of X-ray bursts observed in IGR J17480−2446, together with the unusual spectral and morphological properties, cast doubts on the mechanism powering such bursts. The absence of significant cooling from all the bursts except that from the first brightest one and the unprecedented observations of long trains of bursts with a very short recurrence time led Galloway et al. (2010) to argue that IGR J17480−2446 could be an analogue of GRO J1744−28 in showing Type II X-ray bursts powered by accretion instabilities.

In this paper, we have analysed the bursts shown by IGR J1748−2446 during the first 4 d of *RXTE* observations and we were able to unambiguously measure the recurrence time for a large number of them. We considered the measures of burst fluences and of the *persistent* flux before each burst and we estimated the ratio of the accretion energy liberated to the nuclear energy during the bursts, $\alpha = F_{\rm pers}\, t_{\rm rec}/\mathcal{F}_{\rm burst}$. The average value we have obtained ($\alpha = 96 \pm 3$) strongly favours the hypothesis that these bursts are due to the unstable thermonuclear burning of hydrogen/helium accreted on the NS surface layer. As a matter of fact, under this hypothesis and assuming that all the available hydrogen/helium nuclear fuel is burnt during bursts, such ratio is expected to be $\alpha = Q_{\rm grav}/Q_{\rm nuc}(1+z)$, where $Q_{\rm grav} = GM/R_{\rm NS} = 180$ MeV is the energy liberated per accreted nucleon for a 1.4-$M_\odot$ NS with a radius of 10 km, $1+z = (1-2GM/R_{\rm NS}c^2)^{-1/2}$ measures the gravitational redshift at the NS surface and $Q_{\rm nuc} = 1.6 + 4\langle X\rangle$ MeV per nucleon is the energy released during the thermonuclear burning of a mixture of hydrogen and helium. Here $\langle X\rangle$ is the mass fraction of hydrogen which may not be depleted during the stable burning phase in between bursts and therefore burns with helium during the flash (see e.g. Galloway et al. 2008). The average estimate of $\alpha = 96 \pm 3$ we have given for the bursts shown by IGR J17480−2446 is compatible with the burst being of Type I and indicates $\langle X\rangle = 0.22(2)$ for $(1+z) = 1.31$. In addition, despite the lower statistic of the bursts observed at higher accretion rates, the values of α for the fainter bursts are consistent with the ones found for lower accretion rate regimes (see Fig. 4), even though the statistics are not enough to clearly identify fluctuations of the values of α driven by the variations in $\dot{m}$.

[2] The expected values of $\dot{M}/\dot{M}_{\rm Edd}$ are calculated as $\frac{\dot{M}}{\dot{M}_{\rm Edd}} = \frac{\dot{L}}{\dot{L}_{\rm Edd}}$.

However, the value of α is always close to 96. This further suggests the thermonuclear origin as the most probable for all the bursts. It is worth to note that Type II X-ray bursters, such as MBX 1730−335 and GRO J1744−28, show values of α of the order of unity ($\leq$1.4, Kunieda et al. 1984 and $\leq$4, Lewin et al. 1976). A similar reasoning led Chakraborty & Bhattacharyya (2010) and Chakraborty & Bhattacharyya (2011) to question the interpretation of these bursts in terms of accretion instabilities.[3] We thus conclude that the most probable interpretation for such bursts is in terms of the helium ignition in a layer still partly composed of hydrogen, as the mass-accretion rate is too large to deplete it completely during the phase of the *persistent* emission. This conclusion is further supported by the fact that, as stated by Cumming & Bildsten (2000), for accretion rates $\geq 2 \times 10^{-10}\,\mathrm{M}_{\odot}\,\mathrm{yr}^{-1}$ (see Bildsten 1998 and references therein), the accumulating hydrogen is thermally stable and burns via the hot CNO cycle of Hoyle & Fowler (1965).

Such a conclusion about the composition of the burst material also fits well into theoretical expectations for local accretion rates $0.1\dot{m}_{\rm Edd} \lesssim \dot{m} \lesssim \dot{m}_{\rm Edd}$ (e.g. Fujimoto, Hanawa & Miyaji 1981). The local accretion rate (defined as the total accretion rate divided by the total surface area of the NS) on to the NS in IGR J17480−2446 can be in fact estimated from the persistent X-ray luminosity as $\dot{m} \simeq 0.24(A_{\rm burst}/A_{\rm NS})d_{5.9}^2\dot{m}_{\rm Edd}$, where $A_{\rm NS}$ and $A_{\rm burst}$ are the areas of the NS surface and that of the region where the burst is ignited, respectively. Further evaluating the ignition depth from the burst energetics, $y_{\rm ign} = \mathcal{F}_{\rm burst}(1+z)(d/r)^2 Q_{\rm nuc}^{-1}$, one obtains that the expected recurrence time, $\Delta t = (y_{\rm ign}/\langle\dot{m}\rangle)(1+z)$, fits well the observed values for $Q_{\rm nuc}$ = 2.5 MeV per nucleon. The values that we found are reported in Table 2 and plotted together with the observed recurrence times in Fig. 7.

Based on the results presented above, combined with the considerations we made according to Sztajno et al. (1986) (see Section 2.1), we believe that the bursts from IGR J17480−2446, despite their unusual properties, are Type I bursts and that the ambiguity in their classification possibly arises from the presence of a blackbody component in the persistent flux and the relatively low statistics of the spectrum during the bursts following the first one (see van Paradijs & Lewin 1986).

None of the bursts of IGR J17480−2446 shows photospheric radius expansion. The accurate knowledge of the distance to Terzan 5 makes the estimate of the blackbody radius observed during bursts very appealing (see e.g. Özel, Güver & Psaltis 2009). A detailed spectral analysis of the brightest burst indicates a blackbody radius of $R_{\rm app}^{\infty} = (3.3 \pm 0.5)d_{5.9}$ km. Such a value can be translated into an effective radius, taking into account the spectral hardening induced by the Compton scattering in the NS atmosphere and the gravitational redshift, $R = R_{\rm app}^{\infty} f_{\rm c}^2 (1+z)^{-1}$. For a colour temperature of the order of 2 keV like the one observed, the hardening factor $f_{\rm c}$ was estimated to lie in the range 1.33–1.84 by Madej, Joss & Różańska (2004), with the larger values appropriate for the NS with a smaller gravitational acceleration at the surface. Further taking $1 + z = (1 - 2GM/R_{\rm NS}c^2)^{-1/2} = 1.31$ for a 1.4-$\mathrm{M}_{\odot}$ and 10-km-radius NS, we obtain an estimate of R in the range $\sim$4.5 to $\sim$9 km. The larger value is obtained by taking a large hardening correction factor which is predicted to be valid for a relatively large NS. Also an uncertainty on the distance of the source equal to 0.5 kpc was taken into account. The resulting measure indicates a radius compatible with the typical values for a NS. We also measured (see Section 2.1) the mean apparent radii for selected bursts following the first brightest one (see Table 2), applying the same corrections as that we adopted for the latter. As one can see, also the measures of the radii coming from the fainter bursts confirm that the emitting region during the thermonuclear burst is consistent with the entire NS surface. In addition, this result is in agreement with the fact that the bursts are phase-locked and that there is no variation in the fractional rms associated to the pulse frequency before, during and after the bursts.

Being the NS in IGR J17480−2446 a pulsar, it is worth to ascertain if the magnetic field is able to confine the accreted matter near the magnetic poles. Papitto et al. (2011) estimated an upper limit on the magnetic field of $\sim 2.4 \times 10^{10}$ G, considering the lowest flux at which pulsations have been observed. Following the model described in Brown & Bildsten (1998), it follows that a similar field can confine the accreted matter near a 5-km magnetic cap up to a column density of $\simeq 3 \times 10^8\,\mathrm{g\,cm^{-2}}$ (see Cumming & Bildsten 2000). Such a radius is consistent with the values derived from the spectral analysis (see Section 2.1). Considering the relation given above, the column depth at which the bursts of IGR J17480−2446 ignite can be estimated to lie in the range $0.05 \times 10^8 d_{5.9}^2$–$0.5 \times 10^8 d_{5.9}^2\,\mathrm{g\,cm^{-2}}$, where we have used $Q_{\rm nuc} = 2.5$ MeV per nucleon. It is thus possible that, if the magnetic field is in excess of 10^{10} G, the radius observed during the Type I X-ray bursts reflects only a fraction of the NS surface around the polar caps rather than the entire NS radius. Assuming that the bursts are ignited on to a smaller fraction of the NS surface ($A_{\rm burst}$), the estimate of the ignition depth grows by a factor of $(A_{\rm burst}/A_{\rm NS})^{-2}$, so that values closer to the critical threshold at which helium is thought to start burning unstably on the NS surface, $\geq 6.8 \times 10^8$ (see e.g. Cumming & Bildsten 2000), are obtained as soon as $(A_{\rm burst}/A_{\rm NS}) \leq 0.5$. A confinement of the burst ignition region would straightforwardly help in explaining the very short recurrence times observed in between the fainter bursts. However, as noted before, this interpretation would require a magnetic field larger than the one inferred from the observations. For this reason, the data coming from IGR J17480−2446 point out the existence of an interpretation problem that cannot be completely solved by the currently accepted model describing accretion and thermonuclear production mechanism.

In a few LMXBs, oscillations with a period of 100–150 s [mHz quasi-periodic oscillations (QPOs)] were discovered and associated to the marginally stable nuclear burning on the NS surface (see Heger, Cumming & Woosley 2007; Altamirano et al. 2008). They are observed only in the luminosity range $(0.5\text{–}1.5) \times 10^{37}\,\mathrm{erg\,s^{-1}}$. The small bursts reported here, with a recurrence time between 300–1000 s and associated to a persistent luminosity in the range $(2.2\text{–}7.3) \times 10^{37}\,\mathrm{erg\,s^{-1}}$, are intermediate between full-fledged Type I X-ray bursts and mHz QPOs, providing an ideal laboratory to study the properties of the nuclear burning on the surface of accreting NSs.

The short recurrence time observed in IGR J17480−2446 is particularly interesting for different reasons in addition to the fact that it is the shortest observed until now. Type I X-ray bursts with very short recurrence times have been studied before (see e.g. Keek, Langer & in't Zand 2009; Galloway et al. 2004; Boirin et al. 2007). Even though different ideas have been put forward to explain this rare bursting behaviour, the short recurrence time still remains an open issue in the theory of thermonuclear X-ray bursts. In particular, the extreme behaviour of IGR J17480−2446 puts the source in accretion regimes well beyond the ones currently investigated by the theory of thermonuclear X-ray bursts (see Narayan & Heyl 2003 for a detailed study on the thermonuclear stability of the accreted

[3] Type II bursts observed in MXB 1730−335 (the Rapid Burster) and the accreting X-ray pulsar GRO J1744−28 (Kouveliotou et al. 1996) are thought to be produced by spasmodic episodes of the accretion, probably triggered by the thermal instability at the inner edge of the accretion disc.

matter on to NSs). It is worth to note that before the discovery of IGR J17480−2446 a maximum of four consecutive bursts were observed (see Keek et al. 2010). IGR J17480−2446 has shown several tens of Type I X-ray bursts with the shortest recurrence time ever observed. It has been argued that the short recurrence time could be due to multidimensional effects, such as the confinement of the accreted material to different parts of the surface, possibly as a consequence of a magnetic field (e.g. Melatos & Payne 2005; Lamb et al. 2009). However, this scenario seems to be ruled out for the case of IGR J17480−2446 by the radius measures of the emitting region, which suggest that a region comparable with the whole NS surface burns during the bursts. In addition, the magnetic field of the source appears to be too weak (upper limit $\sim 2.4 \times 10^{10}$) to confine the burning matter to particular regions of the NS surface (see above). Furthermore, the magnetic confinement of the accreted material would not be a plausible explanation for the short recurrence time of 3.8 min observed for 4U 1705−44 (see Keek et al. 2010), which does not show coherent pulsations, but it may show a very soft spectrum, thus indicating a physically weak interacting magnetic field. Also the idea of a burning layer with an unburned layer on top has been investigated. According to Fujimoto (1988), after the first layer flashes, the second layer could be mixed down to the depth where a thermonuclear runaway occurs, thanks to rotational hydrodynamic instabilities (Fujimoto 1988) or instabilities due to a rotationally induced magnetic field (Piro & Bildsten 2007; Keek et al. 2009). Being a pulsar and showing burst oscillations, IGR J17480−2446 belongs to a small group of sources for which the spin period is known and which show short-recurrence-time thermonuclear bursts (see Keek et al. 2010, table 1). All these sources proved to be fast spinning NSs with $\nu_{\rm spin} \geq 500$ Hz. IGR J17480−2446 is the first NS showing short-recurrence-time bursts *and* a low spin frequency (11 Hz). This fact demonstrates that, contrary to what has been thought until now, fast rotation is *not* required for the occurrence of multiple-burst events. For this reason, models predicting multiple burst events produced by the rotationally induced mixing due to the fast spinning frequency should be revised accordingly (see e.g. Fujimoto 1988; Spruit 2002; Keek et al. 2009). Furthermore, the discovery of IGR J17480−2446 and its burst oscillations demonstrate the fact that a fast spin frequency is also not required for burst oscillations to be observed. Since the burst characteristics (profile, rise and decay times) and their energetics do not change even in long-spin-period regimes, we can conclude that the spin frequency of the NS does not affect or only marginally affects the burst production mechanism.

We conclude that, thanks to its rare and unique behaviour, IGR J17480−2446 constitutes an ideal laboratory to investigate in detail the mechanisms that trigger thermonuclear bursts and to test the validity of the theoretical models describing the occurrence of very short recurrence time Type I X-ray bursts.

ACKNOWLEDGMENTS

This work is supported by the Italian Space Agency, ASI- INAF I/088/06/0 contract for High Energy Astrophysics, as well as by the operating programme of Regione Sardegna (European Social Fund 2007-2013), L.R.7/2007 (Promotion of Scientific Research and Technological Innovation in Sardinia). The research leading to these results has received fund from the European Community's Seventh Framework Programme (FP7/2007-2013) under grant agreement number ITN 215212 'Black Hole Universe'. We thank Luigi Stella for carefully reading an earlier version of this work and for useful comments.

REFERENCES

Altamirano D., Watts A., 2010, The Astronomer's Telegram, 2932, 1
Altamirano D., Casella P., Patruno A., Wijnands R., van der Klis M., 2008, ApJ, 674, L45
Altamirano D., Watts A., Linares M., Markwardt C. B., Strohmayer T., Patruno A., 2010, MNRAS, 409, 1136
Bildsten L., 1998, ApJ, 501, L89
Boirin L., Keek L., Méndez M., Cumming A., in't Zand J. J. M., Cottam J., Paerels F., Lewin W. H. G., 2007, A&A, 465, 559
Bordas P. et al., 2010, Astron. Tel., 2919
Brown E. F., Bildsten L., 1998, ApJ, 496, 915
Chakraborty M., Bhattacharyya S., 2010, Aston. Tel., 3044
Chakraborty M., Bhattacharyya S., 2011, ApJ, 730, L23
Cumming A., Bildsten L., 2000, ApJ, 544, 453
Fujimoto M. Y., Hanawa T., Miyaji S., 1981, ApJ, 247, 267
Fujimoto M. Y., 1988, A&A, 198, 163
Galloway D. K., in't Zand J. J. M., 2010, Astron. Tel., 3000
Galloway D. K., Cumming A., Kuulkers E., Bildsten L., Chakrabarty D., Rothschild R. E., 2004, ApJ, 601, 466
Galloway D. K., Muno M. P., Hartman J. M., Psaltis D., Chakrabarty D., 2008, ApJS, 179, 360
Galloway D. K., Lin J., Chakrabarty D., Hartman J. M., 2010, ApJ, 711, L148
Heger A., Cumming A., Woosley S. E., 2007, ApJ, 665, 1311
Hoyle F., Fowler W. A., 1965, in Robinson I., Schild A., Schucking E. L., eds, Proc. 1st Texas Symp. on Relativistic Astrophysics, Quasi-Stellar Sources and Gravitational Collapse. Univ. Chicago Press, Chicago, p. 17
Kaaret P., Morgan E. H., Vanderspek R., Tomsick J. A., 2006, ApJ, 638, 963
Keek L., Langer N., in't Zand J. J. M., 2009, A&A, 502, 871
Keek L., Galloway D. K., in't Zand J. J. M., Heger A., 2010, ApJ, 718, 292
Kouveliotou C., van Paradijs J., Fishman G. J., Briggs M. S., Kommers J., Harmon B. A., Meegan C. A., Lewin W. H. G., 1996, Nat, 379, 799
Kunieda H. et al., 1984, PASJ, 36, 807
Lamb F. K., Boutloukos S., Van Wassenhove S., Chamberlain R. T., Lo K. H., Clare A., Yu W., Miller M. C., 2009, ApJ, 706, 417
Lanzoni B. et al., 2010, ApJ, 717, 653
Leahy D. A., Elsner R. F., Weisskopf M. C., 1983, ApJ, 272, 256
Lewin W. H. G. et al., 1976, ApJ, 207, L95
Madej J., Joss P. C., Różańska A., 2004, ApJ, 602, 904
Markwardt C. B., Swank J. H., 2003, IAU Circ., 8144, 1
Melatos A., Payne D. J. B., 2005, ApJ, 623, 1044
Muno M. P., Chakrabarty D., Galloway D. K., Psaltis D., 2002, ApJ, 580, 1048
Narayan R., Heyl J. S., 2003, ApJ, 599, 419
Özel F., Güver T., Psaltis D., 2009, ApJ, 693, 1775
Papitto A., D'Aì A., Motta S., Riggio A., Burderi L., di Salvo T., Belloni T., Iaria R., 2011, A&A, 526, L3
Piro A. L., Bildsten L., 2007, ApJ, 663, 1252
Pooley D., Homan J., Heinke C., 2010, Astron. Tel., 2974
Poutanen J., Svensson R., 1996, ApJ, 470, 249
Spruit H. C., 2002, A&A, 381, 923
Strohmayer T., Bildsten L., 2006, in Lewin W., van der Klis M., eds, Cambridge Astrophys. Ser. No. 39, Compact Stellar X-ray Sources. Cambridge Univ. Press, Cambridge, p. 113
Strohmayer T. E., Markwardt C. B., 2010, Astron. Tel., 2929
Strohmayer T. E., Markwardt C. B., Swank J. H., in't Zand J., 2003, ApJ, 596, L67
Strohmayer T. E., Markwardt C. B., Pereira D., 2010, Astron. Tel., 2946
Sztajno M., van Paradijs J., Lewin W. H. G., Langmeier A., Trumper J., Pietsch W., 1986, MNRAS, 222, 499
van Paradijs J., Lewin H. G., 1986, A&A, 157, L10
Woosley S. E. et al., 2004, ApJS, 151, 75

This paper has been typeset from a TEX/LATEX file prepared by the author.